
OPTICAL
PROPERTIES

Zeeman Effect and Stark Splitting of the Electronic States of the Rare-Earth Ion in the Paramagnetic Terbium Garnets $Tb_3Ga_5O_{12}$ and $Tb_3Al_5O_{12}$

U. V. Valiev^a, J. B. Gruber^b, D. K. Sardar^b, B. Zandi^c, I. S. Kachur^d, A. K. Mukhammadiev^a,
V. G. Piryatinskaya^d, V. Yu. Sokolov^a, and I. S. Edelman^e

^a National University of Uzbekistan, Tashkent, 700174 Uzbekistan

^b University of Texas at San Antonio, San Antonio, Texas, 78249-0697 United States

^c ARL/Adelphi Laboratory Center, Adelphi, Maryland, 20783-1197 United States

^d Verkin Institute for Low Temperature Physics and Engineering, National Academy of Sciences of Ukraine,
pr. Lenina 47, Kharkov, 61103 Ukraine

^e Kirensky Institute of Physics, Siberian Division, Russian Academy of Sciences,
Akademgorodok, Krasnoyarsk, 660036 Russia

e-mail: ise@iph.krasn.ru

Received November 7, 2005; in final form, April 18, 2006

Abstract—The Zeeman effect in the ${}^7F_6 \rightarrow {}^5D_4$ absorption band of the Tb^{3+} ion in the paramagnetic garnets $Tb_3Ga_5O_{12}$ and $Tb_3Al_5O_{12}$ was studied. The field dependences of the Zeeman splitting of some absorption lines are found to exhibit unusual behavior: as the magnetic field increases, the band splitting decreases rather than increases. Symmetry analysis relates these lines to $4f \rightarrow 4f$ electron transitions of the doublet–quasi-doublet or quasi-doublet–doublet type, for which the field dependences of the splitting differ radically from the well-known field dependences of the Zeeman splitting for quasi-doublet–quasi-doublet or quasi-doublet–singlet transitions in a longitudinal magnetic field.

PACS numbers: 78.20.-e, 78.40.Ha, 75.50.Ee

DOI: 10.1134/S1063783407010167

1. INTRODUCTION

The magnetic properties of rare-earth (RE) garnets, namely, gallates and aluminates, have attracted the attention of researchers for the past several decades due to their wide application as optical insulators, highly effective laser matrices, working elements of integrated-optics and acousto-optics devices, and so on. Among these compounds, terbium garnets are the most promising for creating optical insulators for the visible region due to their high magneto-optic Faraday rotation and low optical absorption. In particular, the authors of [1] discuss various designs of magneto-optical modulators (and optical insulators) that are based on the Faraday effect in RE garnets (including $Tb_3Al_5O_{12}$) and have an efficiency of more than 30 dB in the visible and infrared regions. One of the forbidden (in the electric dipole approximation) $4f \rightarrow 4f$ electron transitions of the Tb^{3+} ion, namely, the ${}^7F_6 \rightarrow {}^5D_4$ transition, falls in this range (470–530 nm). Further progress in the application of terbium garnets in optics requires detailed knowledge of the energy spectrum of the Tb^{3+} ion in the crystal field of a garnet. Therefore, it is a challenge to solve the problem of identifying forbidden $4f \rightarrow 4f$ transitions between the Stark sublevels of the multiplets of the ground $4f^{(n)}$ configuration of non-Kramers RE

ions, including Tb^{3+} . The solution of this problem meets with certain difficulties. One of them is the discrepancy between the numbers of lines usually detected in the absorption and luminescence spectra, and another difficulty is the discrepancy between the experimental and calculated intensity distributions of the spectral lines [2, 3]. These discrepancies are caused by the specific features of the Stark splitting of the energy states of a non-Kramers RE ion in a garnet structure. A low-symmetry crystal field (CF) forms so-called quasi-doublets consisting of two closely spaced Stark singlets, and the gap between these singlets can be extremely small ($\sim 1 \text{ cm}^{-1}$) [2, 4, 5]. Therefore, these quasi-doublets cannot be resolved in optical experiments. On the other hand, the complex behavior of the optical spectra can be caused by the superposition of optical transitions in RE ions occupying crystallographically nonequivalent positions (with symmetry D_2) that differ in terms of the orientation of the local symmetry axes [6] in the cubic structure of a garnet (space group $O_h^{10} - Ia3d$). These difficulties can be overcome in large part when studying $4f \rightarrow 4f$ transitions by Zeeman spectroscopy, since it can distinguish the spectra of magnetoactive ions occupying different crystallographic positions and can determine both the sym-

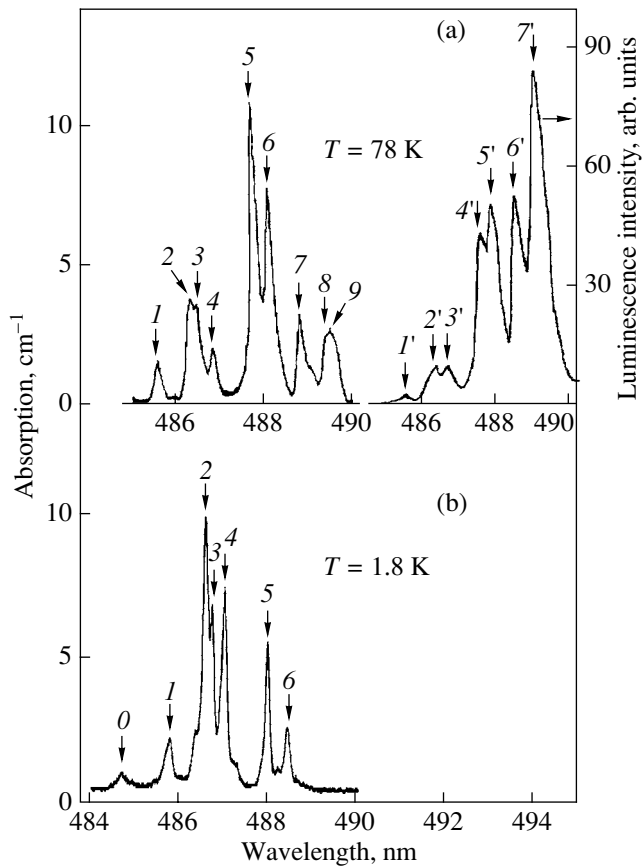


Fig. 1. (a) ${}^7F_6 \rightarrow {}^5D_4$ absorption band spectrum (left) and ${}^5D_4 \rightarrow {}^7F_6$ luminescence band spectrum (right) of TbGaG at $T = 78$ K. (b) ${}^7F_6 \rightarrow {}^5D_4$ absorption band spectrum at $T = 1.8$ K. The characteristic features of the absorption and luminescence bands are indicated by numbered vertical arrows.

metry and character of the Stark splitting of $4f$ electronic states [7, 8].

Zeeman spectroscopy is highly informative due in most part to the relative simplicity of simulating and interpreting the magneto-optical spectra (as compared to optical spectra) as a result of the decreased number of transitions allowed by the symmetry selection rules in non-Kramers RE ions in an applied magnetic field H . Using selection rules for the matrix elements of optical transitions, one can in principle determine the symmetry of the wave functions of the Stark sublevels from which (or to which) forbidden (in the electric dipole approximation) $4f \rightarrow 4f$ transitions occur in non-Kramers RE ions in garnets [9].

The purpose of this work is to study the splitting of the lower Stark sublevels of the 7F_6 and 5D_4 multiplets of the Tb^{3+} ion in crystal and magnetic fields; the transitions between these sublevels form the optical absorption band ${}^7F_6 \rightarrow {}^5D_4$, which is observed in the RE gar-

nets $Tb_3Ga_5O_{12}$ (TbGaG) and $Tb_3Al_5O_{12}$ (TbAG) in the visible region.

2. EXPERIMENTAL

We studied the optical absorption spectrum of the paramagnetic garnet TbGaG for the $4f \rightarrow 4f$ (${}^7F_6 \rightarrow {}^5D_4$) transition of the Tb^{3+} ion in the spectral range 483–493 nm (20300–20750 cm^{-1}) at temperatures $T = 1.8$ and 78 K with a resolution of ≈ 1.0 – 1.5 cm^{-1} at ~ 20400 cm^{-1} . We also recorded the luminescence spectrum of the radiative $4f \rightarrow 4f$ (${}^5D_4 \rightarrow {}^7F_6$) transition at $T = 78$ K in the spectral range 20200–20750 cm^{-1} .

The Zeeman effect (in longitudinal geometry) was studied in the optical absorption spectra of the paramagnetic garnets TbGaG and TbAG at $T = 90$ K in a magnetic field $H = 7$ kOe applied along the [110]- or [001]-type crystallographic directions. To this end, we directly recorded the opposite circularly polarized components σ_{\pm} of absorption lines in a longitudinal magnetic field; these components were separated with a phase-shifting $\lambda/4$ plate and a linear polarizer [9]. A Fresnel rhomb with an angle of $\sim 52^\circ$ made of fused silica served as the $\lambda/4$ plate. The relative error in measuring the absorption coefficients α and α_{\pm} in all experiments did not exceed ~ 2 – 3% .

3. EXPERIMENTAL RESULTS

Figure 1a shows the spectrum of the ${}^7F_6 \rightarrow {}^5D_4$ absorption band in TbGaG recorded in the absence of an applied field at $T = 78$ K and the corresponding luminescence spectrum at the same temperature. The specific features of the absorption and luminescence bands (which are observed at the same energies) are indicated by vertical arrows. As is seen from Fig. 1a, absorption lines 1 and 4–7 are singlets and likely result from the ground state of the 7F_6 multiplet of the Tb^{3+} ion, which is supported by the measured optical absorption of the TbGaG garnet at $T = 1.8$ K (Fig. 1b). The absorption lines at ~ 486.6 nm (~ 20550 cm^{-1}) and ~ 489.5 nm (~ 20428 cm^{-1}) are doublet lines 2, 3 and 8, 9, respectively. Lines 2 and 3 correspond to transitions from the ground state, whereas lines 8 and 9 are related to optical transitions from the excited Stark sublevels of the ground 7F_6 multiplet of the Tb^{3+} ion in the structure of the terbium–gallium garnet.

Figures 2 and 3 show the spectra of the ${}^7F_6 \rightarrow {}^5D_4$ absorption band in isomorphous TbGaG and TbAG crystals recorded for the right-handed (σ_+) and left-handed (σ_-) circular polarizations at $T = 90$ K in a magnetic field $H = 7$ kOe applied along the [110] and [001] crystallographic directions, respectively. As is seen from Fig. 2, absorption lines 5 and 6 in TbGaG undergo noticeable Zeeman splitting of the same sign (the σ_- components shift toward low energies), which is

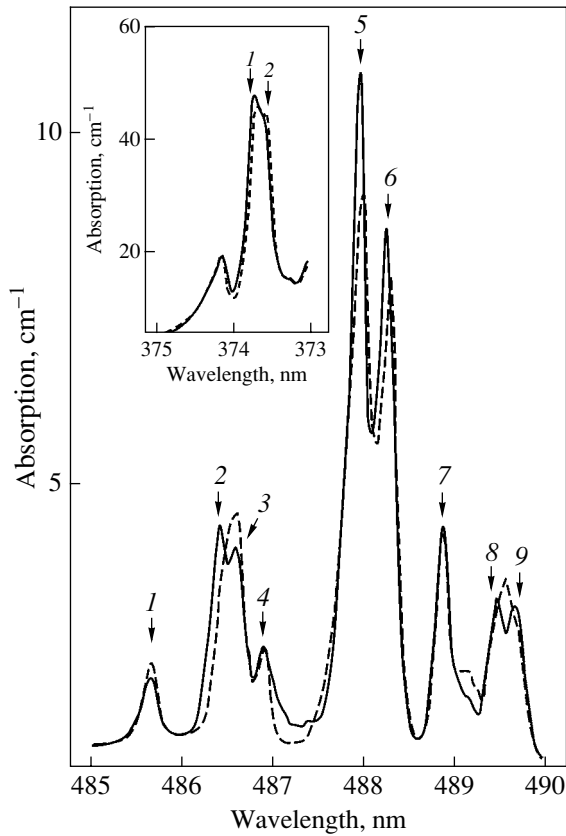


Fig. 2. Spectral dependences of the absorption in the ${}^7F_6 \rightarrow {}^5D_4$ band of TbGaG recorded for the right-handed (σ_+ , solid line) and left-handed (σ_- , dashed line) circular polarizations at $T = 90$ K in a magnetic field $H = 7$ kOe parallel to the [110] crystallographic axis. The inset shows analogous dependences for the doublet absorption line at ~ 373.8 nm (~ 26750 cm^{-1}).

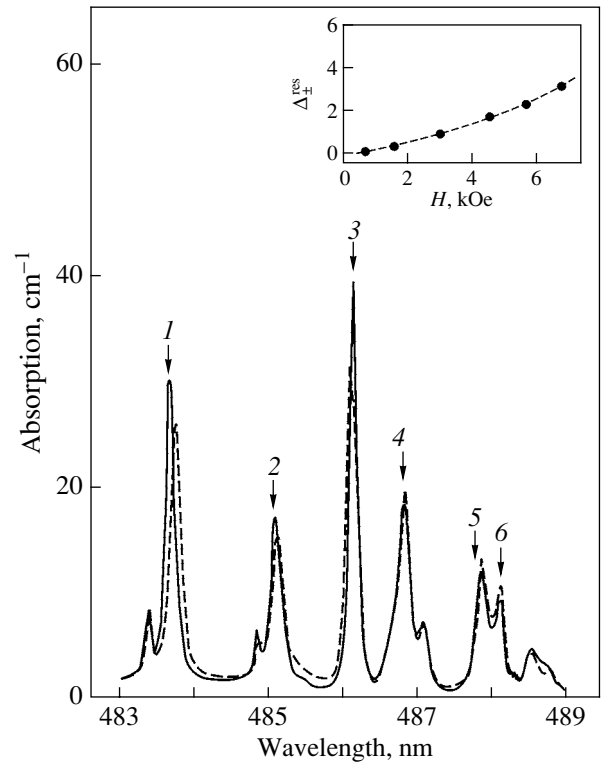


Fig. 3. Spectral dependences of the absorption in the ${}^7F_6 \rightarrow {}^5D_4$ band of TbAG recorded for the right-handed (σ_+ , solid line) and left-handed (σ_- , dashed line) circular polarizations at $T = 90$ K in a magnetic field $H = 7$ kOe parallel to the [001] crystallographic axis. The inset shows the field dependence of the Zeeman splitting $\Delta_{\pm}^{\text{res}}$ of absorption line 1 at $T = 90$ K.

accompanied by a decrease in the intensities of these components in a magnetic field. It is interesting that, although the significant “effective” Zeeman shifts (or splittings) $\Delta_+^{\text{eff}} = \hbar(\omega_+ - \omega_0)$ and $\Delta_-^{\text{eff}} = \hbar(\omega_0 - \omega_-)$ of the resonance frequencies ω_0 of lines 1 and 3 of the ${}^7F_6 \rightarrow {}^5D_4$ absorption band in TbAG have different signs (Fig. 3), the variations in the intensities of these lines in the σ_+ and σ_- polarizations are similar in character to those of lines 5 and 6 in the absorption spectrum of TbGaG (Fig. 2).¹ As the magnetic field increases, the effective splittings Δ_+^{eff} and Δ_-^{eff} (measured for the σ_+ and σ_- polarizations, respectively) of the resonance frequencies of lines 5 and 6 in TbGaG and lines 1 and 3 in TbAG increase and the field dependence of the resulting splitting $\Delta_{\pm}^{\text{res}} = \Delta_+^{\text{eff}} - \Delta_-^{\text{eff}}$ is non-

linear in fields up to 7 kOe (inset to Fig. 3). However, the resonance frequencies of lines 1 and 7 in the spectrum of TbGaG (Fig. 2), as well as lines 2 and 4–6 in TbAG (Fig. 3), shift only weakly (within the optical resolution of the experimental device) with respect to each other in the opposite circular polarizations as the magnetic field increases.

As is seen from Fig. 2, the Zeeman effect in TbGaG in doublet absorption lines 2, 3 and 8, 9 is slightly different. The application of a magnetic field in this case increases the energy spacing between the doublet components for the right-handed circular polarization σ_+ as compared to the spacing Δ_0 measured in a zero magnetic field (cf. Figs. 1, 2). The field dependence of the effective splitting Δ_+^{eff} of absorption doublet 2, 3 at an energy of ~ 20550 cm^{-1} is shown in the inset to Fig. 4. For the opposite circular polarization (σ_-), the components of these doublets move toward each other as the magnetic field increases (for a fixed direction of the field) and virtually completely overlap for $H \approx 7$ kOe.

¹ According to our additional magneto-optical measurements, this behavior is also characteristic of the Zeeman splittings of certain lines in the ${}^5D_4 \rightarrow {}^7F_6$ luminescence band in the terbium-yttrium-aluminum garnet $\text{Tb}_{0.2}\text{Y}_{2.8}\text{Al}_5\text{O}_{12}$ (YAG : Tb^{3+}).

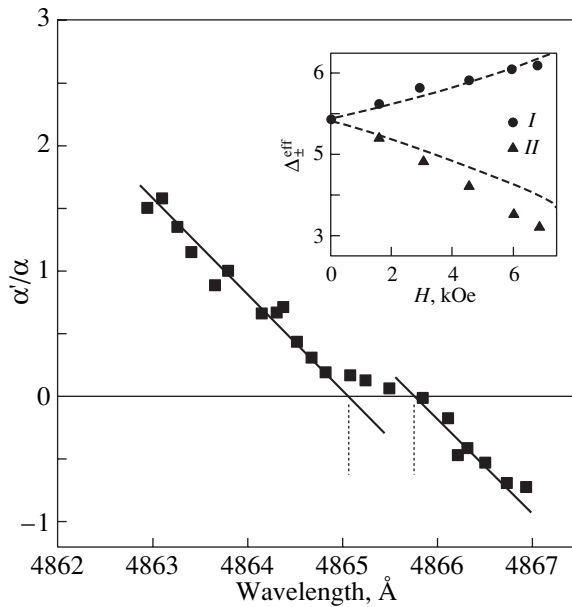


Fig. 4. Dependence of the ratio of the graphical derivative of the absorption band α' to the absorption amplitude α on the light wavelength λ plotted for the complex contour formed by the superposition of closely spaced absorption lines 2 and 3 for the σ polarization in TbGaG in a magnetic field $H = 7$ kOe at $T = 90$ K. The inset shows the field dependences of the Zeeman splittings of absorption lines 2 and 3 for the σ_+ and σ_- polarizations at $T = 90$ K: (I) splitting Δ_+^{eff} and (II) splitting Δ_-^{eff} .

The decomposition of the complex contour of the doublet absorption band for the σ_- polarization into Gaussians [10] makes it possible to obtain the field dependence of the splitting Δ_-^{eff} of the absorption lines for the circular polarization σ_- (inset to Fig. 4).² In this crystal, the optical absorption line at ~ 373.8 nm (~ 26750 cm^{-1}) behaves similarly, as shown in the inset to Fig. 2 for a field $H = 7$ kOe applied along the [110] direction at $T = 90$ K. However, it is difficult to comprehensively study the field dependences of the splitting of this absorption line for the σ_+ and σ_- polarizations, because the doublet group characteristic of this line is poorly resolved in the low-temperature absorption spectra due to the significant overlap of doublet components 1 and 2 in a zero magnetic field.

² In this method, the values of Δ_-^{eff} are determined from the coordinates of the points of intersection of the abscissa axis and the linear dependence of the ratio of the derivative of the absorption band α' to the absorption amplitude α on the light wavelength λ (Fig. 4), $(\alpha'/\alpha)_i = c(\lambda - \lambda_{0i}) + d_i$, where $i = 1, 2$.

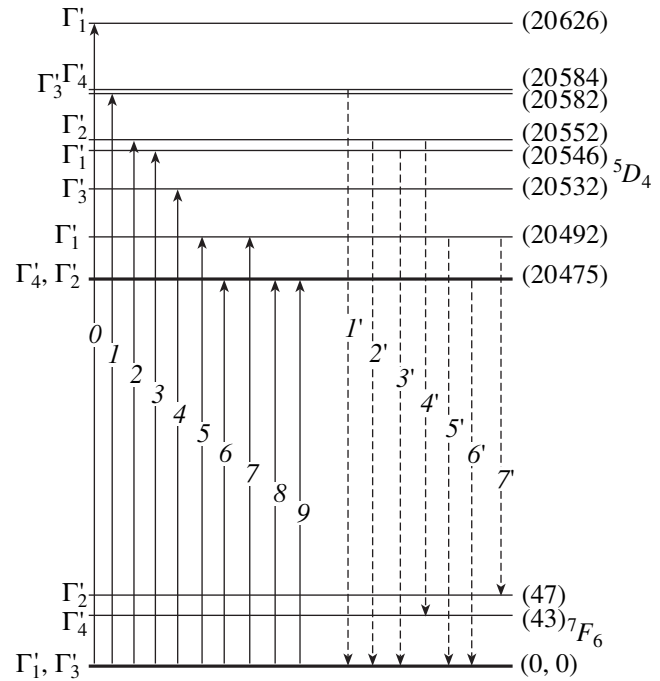


Fig. 5. Scheme of the splittings of the Stark sublevels of the ${}^7F_6 \rightarrow {}^5D_4$ multiplets of the Tb^{3+} ion in TbGaG. Vertical solid lines indicate the symmetry-allowed $4f \rightarrow 4f$ transitions forming the ${}^7F_6 \rightarrow {}^5D_4$ absorption band, and vertical dashed lines indicate the transitions forming the ${}^5D_4 \rightarrow {}^7F_6$ luminescence band at $T = 78$ K. Transition 0 is the allowed transition related to a weak absorption line that is almost unobservable in the experimental spectra recorded at $T = 78$ K.

4. DISCUSSION OF THE RESULTS

In order to identify the lines detected in the absorption and luminescence spectra of the ${}^7F_6 \rightarrow {}^5D_4$ transition, we used the experimental data from [3], our results (Fig. 1), and the numerically calculated Stark sublevels and wave functions of the 7F_6 and 5D_4 multiplets of the Tb^{3+} ion in TbGaG. The results are shown in Fig. 5. It can be seen that absorption lines 2, 3 and 8, 9 are caused by $4f \rightarrow 4f$ transitions between the doublet and quasi-doublet states of the 7F_6 and 5D_4 multiplets. We now consider a fragment (Fig. 6) of the scheme of the magneto-optically active transitions responsible for the Zeeman effect for absorption lines 2 and 3. To construct this scheme, we used the well-known symmetry selection rules for the matrix elements of optical transitions and included the mixing of the quasi-degenerate states of the 7F_6 and 5D_4 multiplets caused by an applied field H [9, 11]. It is significant that, when plotting the transition scheme in Fig. 6, we took into account that a change in the sign of the circular light polarization at a fixed direction of the magnetic field is equivalent to a change in the sign of the applied field at a fixed sign of

circular polarization. A detailed consideration of this scheme demonstrates that, unlike the traditional and easily interpretable picture of the Zeeman splitting of absorption lines 5 and 6 in TbGaG (Fig. 2) and lines 1 and 3 in TbAG (Fig. 3), the aforementioned specific features of the Zeeman effect for absorption lines 2 and 3 in TbGaG at an energy of $\sim 20550 \text{ cm}^{-1}$ and for absorption lines 8 and 9 at an energy of $\sim 20428 \text{ cm}^{-1}$ cannot be explained in terms of the symmetry-allowed optical transitions between the quasi-degenerate states of non-Kramers ions mixed by an applied field [7, 9].

Our analysis of the experimental data shows that the splitting of absorption lines 2 and 3, as well as 8 and 9, can hardly decrease (or become zero) in the scheme of quasi-doublet–quasi-doublet transitions that is traditionally used in the magneto-optics of non-Kramers RE ions [7, 9, 11]. The splitting of the absorption lines can decrease only in the scheme of quasi-doublet–doublet transitions, and this decrease can be caused by the difference in the behaviors of these lines as the magnetization of the RE ion is reversed. Indeed, for the magnetic-field-mixed sublevels of a quasi-doublet, the signs of the angular momentum projections remain unchanged upon magnetization reversal and the magnetic moment of the quasi-doublet is reoriented due to a change in the sign of the field, since this moment is induced by the field (Van Vleck paramagnetism [12]). However, the wave functions of a purely doublet state transform in such a manner that, as the sign of the applied field H changes, the magnetic moment in this state is reoriented due to the inversion of the signs of the angular momentum projections of the sublevels split by the applied field (Fig. 6). Quasi-degenerate states whose behavior during magnetization reversal is similar to that of ordinary (symmetry-degenerate) doublets have been recently detected in the energy spectrum of the multiplets of the ground $4f^{(8)}$ configuration of the Tb^{3+} ion in TbGaG. According to numerically calculated energy spectra and wave functions of the Stark sublevels (see also Appendix), the ground states in the 7F_6 and 5D_4 multiplets are quasi-degenerate states whose “initial” splittings Δ_0 ($\leq 0.1 \text{ cm}^{-1}$) in a CF of symmetry D_2 are significantly smaller than the Zeeman splittings (i.e., $\Delta_0 \ll g_{\parallel} \mu_B H$, where g_{\parallel} is the quasi-doublet g -tensor component parallel to the field). The wave functions of these states are transformed according to the irreducible representations of group D_2 , namely, (Γ'_1, Γ'_3) and (Γ'_4, Γ'_2) , respectively. The field dependence of the Zeeman splitting in them in relatively low magnetic fields (up to 10 kOe) is simulated like that of purely doublet states; therefore, the (Γ'_1, Γ'_3) and (Γ'_4, Γ'_2) states can be identified with symmetry-degenerate doublets whose sublevels are described by the wave functions $|6, \pm 6\rangle$ and $|4, \pm 3\rangle$, respectively, in the local coordinate system of the Tb^{3+} ion in a garnet structure (see Appendix). Then, for magneto-optically active transi-

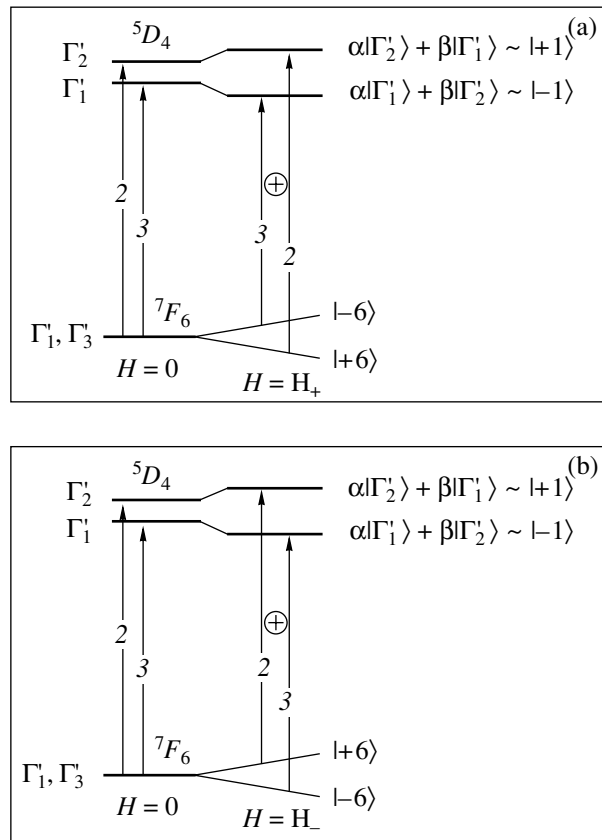


Fig. 6. Fragment of a scheme of the magneto-optically active transitions responsible for the Zeeman effect for absorption lines 2 and 3 in the ${}^7F_6 \rightarrow {}^5D_4$ absorption band of TbGaG in a magnetic field applied (a) along the direction of propagation of light and (b) in the opposite direction.

tions [9], the (Γ'_1, Γ'_3) and (Γ'_4, Γ'_2) doublet states combine with the applied-field-mixed (Γ'_1, Γ'_2) and (Γ'_1, Γ'_4) quasi-doublet states, respectively, according to the selection rules. In this case, the inversion of the Zeeman sublevels of the doublets caused by magnetization reversal leads to a transition scheme that actualizes the case of interest where the splitting of absorption lines 2 and 3, as well as that of lines 8 and 9, decreases significantly (see Fig. 6 and Appendix).

This scheme is supported by the consideration of the Zeeman effect for absorption lines 2 and 3 related to the $4f \rightarrow 4f$ transition ${}^7F_6(\Gamma'_1, \Gamma'_3) \rightarrow {}^5D_4(\Gamma'_1, \Gamma'_2)$ in TbGaG performed with allowance for the scheme of optical transitions shown in Fig. 6. Since the wave functions of the ground state of the 7F_6 multiplet in TbGaG transform according to the irreducible representations Γ'_1 and Γ'_3 of group D_2 and the wave functions of the excited quasi-doublet state of the 5D_4 multiplet transform according to the irreducible representations Γ'_1

and Γ'_2 . the splittings Δ_+ (for circular polarization σ_+) of the doublet and quasi-doublet states that combine in the ${}^7F_6(\Gamma'_1, \Gamma'_3) \rightarrow {}^5D_4(\Gamma'_1, \Gamma'_2)$ transition for one of the nonequivalent positions of the RE ion in gallate [2, 6] can be written as

$$\Delta_+ = \sqrt{\Delta_0^2 + \mu_B^2 H_z^2 g_z^2 + \mu_B^2 H_y^2 g_y^2}, \quad (1)$$

where g_z and g_y are g -tensor components of the doublet and quasi-doublet, respectively; Δ_0 is the initial splitting of the (Γ'_1, Γ'_2) quasi-doublet in the CF; H_z and H_y are the projections of the applied field on the axes of the local coordinate system of the RE ion; and μ_B is the Bohr magneton. In terms of the same designations and for the same RE ion position [2, 6], the splittings Δ_- of the doublet and quasi-doublet states that combine in the circular polarization σ_- can be written as

$$\Delta_- = \sqrt{\Delta_0^2 - (\mu_B^2 H_z^2 g_z^2 - \mu_B^2 H_y^2 g_y^2)}. \quad (2)$$

We now sum Eqs. (1) and (2) over all groups of nonequivalent RE ions in the garnet, average them, and find the effective Δ_+^{eff} and Δ_-^{eff} splittings involved in the optical transitions between the doublet and quasi-doublet states for the σ_+ and σ_- polarizations, respectively, when a magnetic field H is applied along the [110] direction:

$$\Delta_+^{\text{eff}}(H) = \frac{1}{6} \left[\Delta_0 + g_z \mu_B H + \sqrt{\Delta_0^2 + g_y^2 \mu_B^2 H^2} + 4 \sqrt{\Delta_0^2 + \mu_B^2 H^2 \frac{(g_y^2 + g_z^2)}{4}} \right], \quad (3)$$

$$\Delta_-^{\text{eff}}(H) = \frac{1}{6} \left[\Delta_0 - g_z \mu_B H + \sqrt{\Delta_0^2 + g_y^2 \mu_B^2 H^2} + 4 \sqrt{\Delta_0^2 - \mu_B^2 H^2 \frac{(g_y^2 - g_z^2)}{4}} \right]. \quad (4)$$

We use Eqs. (3) and (4) to fit the experimental field dependences of the effective splittings Δ_+^{eff} and Δ_-^{eff} (Fig. 4) for absorption lines 2 and 3 in fields up to 7 kOe. Using the initial (crystal-field) splitting ($\Delta_0 = 5.65 \text{ cm}^{-1}$) of the (Γ'_1, Γ'_2) quasi-doublet, we can easily determine the g -tensor components of the (Γ'_1, Γ'_3) doublet and (Γ'_1, Γ'_2) quasi-doublet to be $g_z = 18.0$ and $g_y = 6.0$, respectively. By analyzing analogous experimental data for absorption lines 8 and 9 caused by the ${}^7F_6(\Gamma'_1, \Gamma'_4) \rightarrow {}^5D_4(\Gamma'_4, \Gamma'_2)$ transition, we find the g -tensor components of the (Γ'_1, Γ'_4) quasi-doublet and

(Γ'_4, Γ'_2) doublet to be $g_x = 15.0$ and $g_z = 8.5$, respectively. Here, we used an experimental crystal-field splitting of the (Γ'_1, Γ'_4) quasi-doublet $\Delta_0 = 4.5 \text{ cm}^{-1}$. Note that the field dependences of the effective splittings Δ_+^{eff} and Δ_-^{eff} as calculated from Eqs. (3) and (4) are almost linear in fields up to 7 kOe and that they satisfactorily describe the experimental curves (see inset to Fig. 4).

Theoretically, the Zeeman splittings of the quasi-degenerate states in the non-Kramers RE ion considered above are determined by the nonzero components of the effective g tensor [7, 12]:

$$g_k = 2g_J \langle \Gamma'_i | \hat{J}_k | \Gamma'_j \rangle, \quad (5)$$

where \hat{J}_k is the k th component of the total angular momentum operator of the RE ion, g_J is the Landé splitting factor of the multiplet, and $i \neq j$. Computations performed using Eq. (5) and the calculated wave functions of the Stark sublevels of the quasi-degenerate states of the 7F_6 and 5D_4 multiplets (see also Appendix) demonstrate that the g -tensor z components of the (Γ'_1, Γ'_3) and (Γ'_4, Γ'_2) doublet states are equal to $g_z = 17.93$ and $g_z = 8.54$, respectively, and that the g -tensor y and x components of the (Γ'_1, Γ'_2) and (Γ'_1, Γ'_4) quasi-doublet states are $g_y = 5.95$ and $g_x = 15.54$, respectively. The experimental and calculated g -tensor components of the quasi-degenerate states of the 7F_6 and 5D_4 multiplets are seen to agree well, which supports the validity of our model; this model relates the unusual behavior of the Zeeman effect to the specific features of the Stark splitting of the energy spectrum of the Tb^{3+} ion in a CF of symmetry D_2 in TbGaG .

In concluding this section, we note that the longitudinal Zeeman effect is highly sensitive to the manner in which the odd CF components mix the states of the ground $4f^{(n)}$ configuration of the Tb^{3+} ion with the states of electron configurations of opposite parity ($4f^{(n-1)}5d$ or $4f^{(n-1)}5g$) in the gallate garnet when the forbiddenness of the $4f \rightarrow 4f$ transition is lifted (as compared to the isomorphic structure of the aluminate garnet). Indeed, the specific features of the Zeeman effect for $4f \rightarrow 4f$ transitions in the ${}^7F_6 \rightarrow {}^5D_4$ absorption band of TbAG can be explained by an admixture of the mixed excited $4f^{(n-1)}5d$ configuration to the states of the ground $4f^{(n)}$ configuration of the Tb^{3+} ion [9], whereas the unusual behavior of the field dependences of the Zeeman effect in TbGaG can only be explained under the assumption that the $4f^{(n-1)}5d$ and $4f^{(n-1)}5g$ configurations are admixed with the ground configuration in almost equal proportions (see also Appendix).

APPENDIX

To interpret the results of the magneto-optical and optical studies of the ${}^7F_6 \rightarrow {}^5D_4$ absorption band of the non-Kramers Tb^{3+} ion in TbGaG , we used numerically calculated wave functions and energies of the Stark sublevels of the 5D_4 and 7F_6 multiplets of the Tb^{3+} ion occupying one of the nonequivalent positions (which is characterized by symmetry group D_2) in the structure of the TbGaG garnet. The calculations are based on the complete CF Hamiltonian

$$\hat{H}_{\text{cr}} = \sum_{k,q} B_{kq} (C_k^q + C_k^{-q}), \quad (\text{A1})$$

where nine CF parameters B_{kq} ($k = 2, 4, 6; q = 0, 2, 4, 6$) are nonzero for symmetry D_2 and C_k^q are irreducible tensor operators [2, 12]. For the numerical calculations, the initial data are taken to be the set of CF parameters B_{kq} obtained by computing lattice sums and the results of the optical studies of terbium gallate garnets borrowed from [3]. To classify (in terms of symmetry) the calculated Stark energy sublevels of the 7F_6 and 5D_4 multiplets and the corresponding wave functions written in the simple basis $|J, M\rangle$ [2, 12], we used the irreducible representations Γ'_i ($i = 1, 2, 3, 4$) of symmetry group D_2 in a local coordinate system of the RE ion where the y' and z' axes are directed along twofold axes of the $[110]$ type and the x' axis is parallel to a crystallographic direction of the $[100]$ type [2, 6].

Let us consider a model of the $4f \rightarrow 4f$ transition between the doublet (Γ'_1, Γ'_3) and quasi-doublet (Γ'_1, Γ'_2) states associated with the ${}^7F_6 \rightarrow {}^5D_4$ absorption band of the non-Kramers Tb^{3+} ion (see Figs. 2, 6). The numerically calculated wave functions of the doublet (which is equivalent to a symmetry-degenerate doublet in terms of its properties) can be described by linear combinations of the spherical harmonics $|6, \pm 6\rangle$, and the wave functions of the quasi-doublet can be represented as

$$\begin{aligned} {}^7F_6|\Gamma'_1\rangle &= 0.7044(|6, +6\rangle + |6, -6\rangle), \\ {}^7F_6|\Gamma'_3\rangle &= 0.703(|6, +6\rangle - |6, -6\rangle), \\ {}^5D_4|\Gamma'_1\rangle &= 0.1223(|4, +2\rangle + |4, -2\rangle) \\ &- 0.5709(|4, +4\rangle + |4, -4\rangle) - 0.5642|4, +0\rangle, \\ {}^5D_4|\Gamma'_2\rangle &= -0.7025(|4, +1\rangle - |4, -1\rangle) \\ &- 0.0724(|4, +3\rangle - |4, -3\rangle). \end{aligned} \quad (\text{A2})$$

A longitudinal magnetic field H splits the doublet states (Γ'_1, Γ'_3) and mixes the quasi-doublet states (Γ'_1, Γ'_2) as shown in Fig. 6. In this case, the matrix elements of the symmetry-allowed [9] optical transitions

between the Zeeman sublevels of the ‘‘accidental’’ doublet (Γ'_1, Γ'_3) and the quasi-doublet (Γ'_1, Γ'_2) for the orthogonal circular polarizations can be found using the well-known expression for the matrix element of a parity-forbidden $4f \rightarrow 4f$ transition in the low-symmetry weak-CF approximation [13]:

$$\begin{aligned} P_q \equiv \langle i|\hat{P}_q^{(1)}|j\rangle &= \sum_{t=3,5,7} \sum_{p=2,4,6} \sum_{M,M'}^{p < t} a_M^{(i)} b_{M'}^{(j)} (-1)^{J-M} \\ &\times \sum_{\lambda=2,4,6} (2\lambda+1) \Gamma^{(\lambda)} B_p^t \Xi(t, \lambda) \\ &\times \left[\begin{pmatrix} J' & J & \lambda \\ M' & -M & p+q \end{pmatrix} \begin{pmatrix} t & 1 & \lambda \\ p & q & -(p+q) \end{pmatrix} \right. \\ &\left. + \begin{pmatrix} J' & J & \lambda \\ M' & -M & q-p \end{pmatrix} \begin{pmatrix} t & 1 & \lambda \\ -p & q & p-q \end{pmatrix} \right], \end{aligned} \quad (\text{A3})$$

$$q = \pm 1, \quad |i\rangle = \sum_M a_M^{(i)} |J, M\rangle, \quad |j\rangle = \sum_M b_M^{(j)} |J', M'\rangle.$$

The designations in Eq. (A3) coincide with those used in [9, 13]. Using the selection rules for the $3j$ symbols [14] in Eq. (A3) and taking into account the admixture (due to the odd CF components) of the states of the mixed excited configurations $4f^{(7)}5d$ ($l' = 2$) and $4f^{(7)}5g$ ($l' = 4$) to the states of the ground configuration $4f^{(8)}$ ($l = 3$) of the Tb^{3+} ion, we can readily find the relevant matrix elements of the $4f \rightarrow 4f$ transitions in a magnetic field $H = H_+$ for the right-handed circular polarization ($q = +1$):

$$\begin{aligned} &\langle +6|\hat{P}_{+1}^{(1)}|\Gamma'_2\rangle \\ &\sim \begin{pmatrix} 4 & 6 & 6 \\ +1 & -(+6) & 5 \end{pmatrix} \begin{pmatrix} 5 & 1 & 6 \\ 4 & 1 & -5 \end{pmatrix} B_4^5 \Xi(5, 6) \end{aligned}$$

for absorption line 2 at $\lambda = 6$, $t = 5$, and $p = 4$ and

$$\begin{aligned} &\langle -6|\hat{P}_{+1}^{(1)}|\Gamma'_1 + \alpha\Gamma'_2\rangle \\ &\sim \begin{pmatrix} 4 & 6 & 6 \\ -1 & -(-6) & -5 \end{pmatrix} \begin{pmatrix} 7 & 1 & 6 \\ -6 & 1 & 5 \end{pmatrix} B_6^7 \Xi(7, 6) \end{aligned}$$

for absorption line 3 at $\lambda = 6$, $t = 7$, and $p = 6$. Under the action of the time-reversal operator (which is equivalent to a change in the sign of the applied field $H \rightarrow -H$ at a fixed circular polarization of light), the wave functions of the quasi-doublet remain unchanged, whereas the wave functions of the doublet transform into each other (Fig. 6). This difference in the mechanism of magnetization reversal between the quasi-doublet and pure doublet state results in a substantial change in the

pattern of the $4f \rightarrow 4f$ transitions between the Zeeman sublevels of the “accidental” doublet (Γ_1', Γ_3') and the quasi-doublet (Γ_1', Γ_2') in an applied field of opposite sign ($H = -H$) at the same circular polarization ($q = +1$), whereas the matrix elements of the optical transitions remain virtually unchanged.

An analysis of the Zeeman effect patterns shown in Figs. 2 and 3 demonstrates that, in an applied field H_+ , the energy spacing between the absorption lines related to the $4f \rightarrow 4f$ transitions under study increases substantially. However, as the sign of the magnetic field changes ($H \rightarrow -H$) at a fixed circular polarization of light, the absorption lines begin to shift toward each other and the splitting becomes zero at a field $H_-^* = 7$ kOe.

It is significant that the experimentally observed (Fig. 2) and theoretically explained field dependences of the Zeeman effect for the $4f \rightarrow 4f$ transitions of the doublet \rightarrow quasi-doublet and quasi-doublet \rightarrow doublet type differ radically from the well-known field dependences of the Zeeman splitting for the quasi-doublet \rightarrow quasi-doublet (and quasi-doublet \rightarrow singlet) transitions in a longitudinal magnetic field (Fig. 3).

ACKNOWLEDGMENTS

This work was supported in part by the Science and Technology Center of Uzbekistan, project no. F-2.1.38.

REFERENCES

1. A. K. Zvezdin and A. V. Kotov, *Modern Magneto-Optics and Magneto-Optical Materials* (Institute of Physics, Bristol, United Kingdom, 1997).

2. R. Bayerer, J. Heber, and D. Mateika, *Z. Phys. B: Condens. Matter* **64**, 201 (1986).
3. B. D. Joshi and A. G. Page, *J. Lumin.* **15**, 29 (1977).
4. R. Z. Levitin, A. K. Zvezdin, M. von Ortenberg, V. V. Platonov, V. I. Plis, A. I. Popov, N. Puhmann, and O. M. Tatsenko, *Fiz. Tverd. Tela (St. Petersburg)* **44** (11), 2013 (2002) [*Phys. Solid State* **44** (11), 2107 (2004)].
5. V. I. Plis and A. I. Popov, *Fiz. Tverd. Tela (St. Petersburg)* **46** (12), 2155 (2004) [*Phys. Solid State* **46** (12), 2229 (2004)].
6. H. Gross, J. Neukum, J. Heber, D. Mateika, and Tang Xiao, *Phys. Rev. B: Condens. Matter* **48**, 9264 (1993).
7. N. P. Kolmakova, S. V. Koptsik, G. S. Krinchik, V. N. Orlov, and A. Ya. Sarantsev, *Fiz. Tverd. Tela (Leningrad)* **32** (5), 1406 (1990) [*Sov. Phys. Solid State* **32** (5), 821 (1990)].
8. T. Kambara, W. J. Haas, F. H. Spedding, and R. H. Good, *J. Chem. Phys.* **58**, 672 (1973).
9. U. V. Valiev, J. B. Gruber, B. Zandi, U. R. Rustamov, A. S. Rakhmatov, D. R. Dzhuraev, and N. M. Narzullaev, *Phys. Status Solidi B* **242**, 933 (2005).
10. J. Badoz, M. Billardon, A. C. Boccara, and B. Briat, *Symp. Faraday Soc.* **3**, 27 (1969).
11. P. J. Stephens, *Adv. Chem. Phys.* **35**, 197 (1976).
12. A. K. Zvezdin, V. M. Matveev, A. A. Mukhin, and A. I. Popov, *Rare-Earth Ions in Magneto-Ordered Crystals* (Nauka, Moscow, 1985) [in Russian].
13. N. P. Kolmakova, S. V. Koptsik, G. S. Krinchik, and A. Ya. Sarantsev, *Fiz. Tverd. Tela (Leningrad)* **33** (9), 2674 (1991) [*Sov. Phys. Solid State* **33** (9), 1510 (1991)].
14. I. I. Sobelman, *Introduction to the Theory of Atomic Spectra* (Nauka, Moscow, 1977; Pergamon, Oxford, 1972).

Translated by K. Shakhlevich